HIGH INTENSITY BEAM TRIAL OF UP TO 540 KW IN J-PARC RCS

H. Hotchi#, H. Harada, N. Hayashi, M. Kinsho, P.K. Saha, Y. Shobuda, F. Tamura, K. Yamamoto, M. Yamamoto, and M. Yoshimoto, J-PARC, JAEA, Tokai, Ibaraki, 319-1195, Japan
Y. Irie, KEK, Tsukuba, Ibaraki, 305-0801, Japan
S. Kato, Graduate School of Science, Tohoku University, Sendai, Miyagi, 980-8578, Japan

Abstract

The beam power ramp-up of the J-PARC RCS has steadily proceeded since the startup of user program in December 2008. In this process, we have recently performed a high intensity beam trial of up to 540 kW. In this paper, beam intensity dependence and injection painting parameter dependence of beam loss, observed in this beam experiment, will be discussed with the corresponding numerical simulation results.

INTRODUCTION

The J-PARC 3-GeV Rapid Cycling Synchrotron (RCS) is a high-power proton driver with two functions; one as a proton source to produce pulsed muons and neutrons at the Materials and Life Science Experimental Facility and another as an injector to the following 50-GeV Main Ring Synchrotron. RCS accelerates protons injected from the linac up to 3 GeV with a repetition rate of 25 Hz. Our final goal is to achieve 1 MW output beam power, which would be the highest level in the world.

The J-PARC beam commissioning began in November 2006 from the linac to the downstream facilities. RCS was beam commissioned in October 2007. Following the initial beam tuning [1], RCS was made available for user operation in December 2008 with an output beam power of 4 kW. Since then, the beam power ramp-up of RCS has steadily proceeded following the progression in beam tuning and hardware improvements [2][3]. The current injection energy is 181 MeV. With this injection energy, RCS is now stably providing more than 300 kW output beam power for users. The linac will be upgraded in the 2013 and 2014 summer shutdown period; the output energy will be improved from 181 MeV to 400 MeV with the addition of an ACS linac in 2013, and the maximum peak current will be increased from 30 mA to 50 mA by replacing the front-end system (IS and RFQ) in 2014. After that, we are to aim at our final goal of the 1 MW design output beam power. Thus, RCS is now in transition from the initial commissioning phase to the final stage aiming at the 1 MW design output beam power.

Recently we have performed a high intensity beam trial of up to 540 kW (4.5e13 protons per pulse) with the injection energy of 181 MeV. The space charge effect at injection in this beam intensity is 1.6 times higher than that in the 1 MW design beam operation with the higher injection energy of 400 MeV as per the $\beta^2\gamma^3$ scaling law. Therefore, the experimental data will serve as a valuable benchmark test for discussing the further RCS power upgrade scenario in future as well as for realizing the 1 MW design beam operation. In this paper, beam intensity dependence and injection painting parameter dependence of beam loss, observed in this high intensity beam trial, will be discussed with the corresponding numerical simulation results (simulation code: Simpsons [4]).

#hotchi.hideaki@jaea.go.jp

BEAM LOSS REDUCTION BY INJECTION PAINTING

The most important issues in increasing the output beam power are the control and minimization of beam loss to keep machine activation within the permissible level. There are many sources of beam loss, in which the most critical one is the space charge effect in the low energy region. It generally imposes a major performance limit on high-power proton synchrotrons. To alleviate this, the RCS adopts transverse and longitudinal injection painting technique [5].

The left table in Fig. 1 shows injection painting parameters applied in this experiment. In transverse painting, correlated painting with the painting emittance of up to 216π mm mrad (ε_{tp}) was used. On the other hand, in longitudinal painting [6][7], the momentum offset injection of 0 to −0.2% (Δp/p) was employed in combination with the superposition of second harmonic rf with an amplitude of 80% (V_2/V_1) of the fundamental rf. In addition, the phase sweep from −100 to 0 degrees (ϕ_2) of the second harmonic rf was applied during injection, which enables further bunch distribution control through a dynamical change of the rf bucket potential.

ID	ε_{tp} (π mm mrad)	V_2/V_1 (%)	ϕ_2 (deg)	Δp/p (%)
1	-	-	-	-
2	100	-	-	-
3	-	80	-100	-0.0
4	-	80	-100	-0.1
5	-	80	-100	-0.2
6	100	80	-100	-0.0
7	100	80	-100	-0.1
8	100	80	-100	-0.2
9	150	80	-100	-0.2
10	200	80	-100	-0.2
11	216	80	-100	-0.2

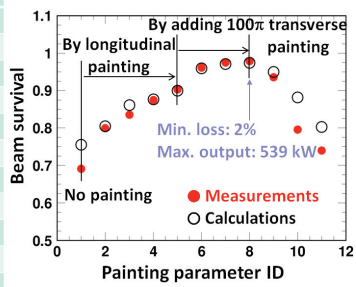

Figure 1: (Left) Injection painting parameters. (Right) Painting parameter dependence of beam survival measured for 540 kW intensity beam with systematic combinations of transverse and longitudinal painting listed in the left table.

The right plot in Fig. 1 shows beam survivals measured for 540 kW intensity beam with systematic combinations of transverse and longitudinal painting listed in the left

table in Fig. 1. As shown in the figure, large beam loss of 30% was observed for the case with no painting (ID 1). But this beam loss was drastically decreased to 2% by longitudinal painting (ID 1 to ID 5) and by adding 100π-mm-mrad transverse painting (ID 5 to ID 8).

In Figure 1, the open circles show the corresponding numerical simulation results. They well reproduce the trend of measured painting parameter dependence of beam loss. Figure 2 shows tune footprints calculated at the end of injection for the parameter IDs 1 and 8. In the case of ID 1 with no painting, a core part of the beam particles crosses the low-order systematic resonance lines such as $\nu_{x,y}=6$, $2\nu_x+2\nu_y=24$, and $\nu_x+2\nu_y=18$, where the particles suffer from emittance dilutions. This is the main cause of 30% large beam loss observed for ID 1, and the beam loss reduction achieved by ID 8 can be interpreted as the outcome of the space charge mitigation led through the charge density control by injection painting and its resultant mitigation of the influence from the betatron resonances.

In the following section, possible mechanisms for the remaining 2% beam loss will be discussed through the detailed comparison between experiment and numerical simulation.

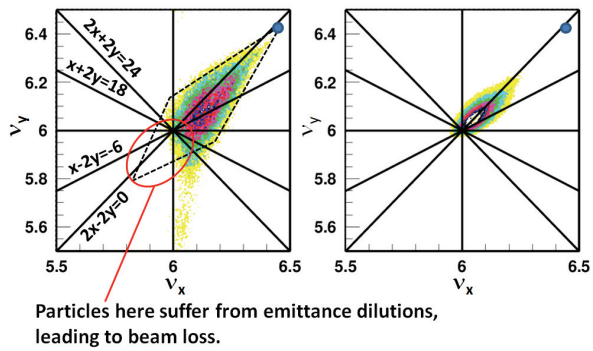

Figure 2: Tune footprints calculated at the end of injection for the parameter IDs 1 (left) and 8 (right).

INTENSITY DEPENDENCE OF BEAM LOSS AND ITS BEAM LOSS MECHANISM

Next, we measured the intensity dependence of beam loss over the range from 100 kW to 540 kW, where the beam intensity was adjusted by changing the injection pulse length from 100 μs to 500 μs. In this measurement, the injection painting parameter of ID 8 was employed, which gave the beam loss minimum (2%) for 540 kW intensity beam, as mentioned in the last section.

The upper plot in Fig. 3 shows the scintillation type beam loss monitor signal for the first 6 ms measured at the collimator section for 100-to-540-kW intensity beams, while the lower plot in Fig. 3 shows the integration of the beam loss monitor signals where the vertical axis is normalized to be beam loss. As shown in the figure, the beam loss appears only for the first 4 ms in the low energy region, and has characteristic two peak structures; (A) and (B). Figure 4 shows the corresponding numerical simulation results. They well reproduce the measured intensity dependence and time structure of beam loss.

From the numerical simulations, the first peak structure in the beam loss monitor signal (A) was identified as foil scattering beam loss during charge-exchange (H^- to proton) injection. As shown in Fig. 3 and 4, the beam loss observed for 100-to-300 kW intensity beams is only from foil scattering. It means that the beam loss is well minimized up to 300 kW intensity beam.

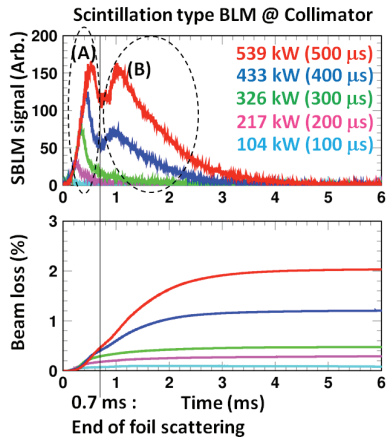

Figure 3: (Upper) Scintillation type beam loss monitor signal for the first 6 ms measured at the collimator section for 100-to-540-kW intensity beams. (Lower) Integration of the beam loss monitor signals, where the vertical axis is normalized to be beam loss.

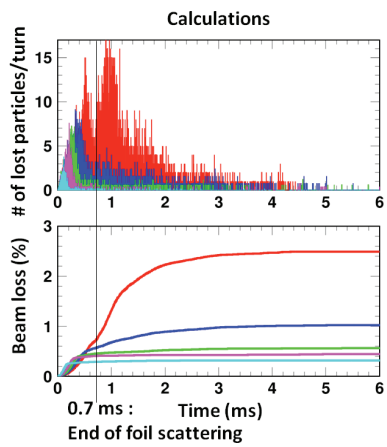

Figure 4: Numerical simulation results corresponding to the experimental results in 3.

On the other hand, the second peak structure in the beam loss monitor signal (B) observed only for higher intensity beams was identified as the beam loss arising from a 100-kHz dipole field ripple induced by the injection bump field. Figure 5 shows a FFT analysis result of BPM signal, in which we can see another significant peak in addition to the revolution frequency and betatron side-band peaks. This peak corresponds to the side-band peak excited by the 100-kHz ripple, which exists only when the injection bump is active (1 ms period from the

ISBN 978-3-95450-122-9

beginning of injection). Figure 6 shows tune footprints calculated at the end of injection for each intensity beam. In the tune space, the 100-kHz ripple makes additional betatron resonances at 0.2. The current operating point is set at (6.45, 6.42), which is far from the resonance lines. But a part of beam particles reaches to the resonance lines due to the space-charge tune depression, where the effect of the field ripple builds up, leading to the emittance growth. As shown in Fig. 6, the situation of resonance crossing is different depending on the beam intensity. For the lower intensity beam, a core part of the beam is on the resonances, while for the higher intensity beam, a tail part of the beam is on the lines. The situation for higher intensity beams is more critical in terms of halo/tail formation and its resultant beam loss, because the 100-kHz ripple directly affects a tail part of the beam. As shown in Fig. 7, larger beam halo/tail formation takes place for higher intensity beams. This is the reason why the second beam loss structure (B) is observed only for higher intensity beams.

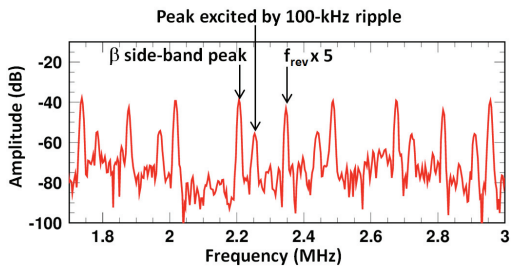

Figure 5: FFT spectrum of BPM signal (horizontal) when the injection bump is active.

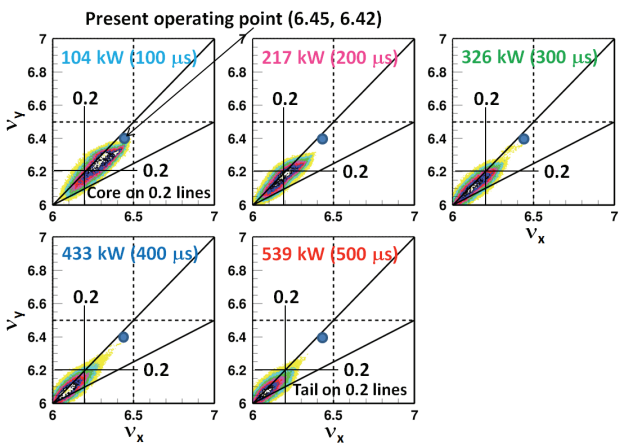

Figure 6: Tune footprint calculated at the end of injection for each intensity beam. In the tune space, the 100-kHz ripple makes additional betatron resonances at 0.2.

This 100-kHz dipole field ripple is estimated to be from that the ripple frequency of the injection bump field resonates with the resonant frequency of the rf shield with capacitor on the ceramics vacuum chamber [8]. In order to mitigate the effect of this ripple, we plan to install the new ceramics chamber with modified rf-shield structure in this summer maintenance period. If this attempt works well, the excess beam loss of 2% occurring for 540 kW intensity beam will be decreased to less than 1%.

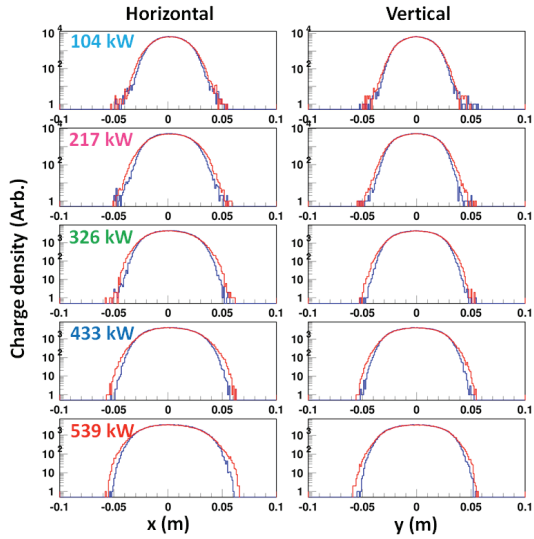

Figure 7: Transverse beam profile calculated at the end of injection for each intensity beam without (blue) and with (red) the 100-kHz ripple.

SUMMARY

We have successfully performed a high intensity beam trial of up to 540 kW. The beam loss for 540 kW intensity beam was well reduced from 30% to 2% by injection painting. This remaining beam loss of 2%, arising from foil scattering and 100-kHz field ripple induced by injection bump field, corresponds to 650 W in power, which is still less than 1/6 of the current collimator capability of 4 kW.

The numerical simulation well reproduced the experimental results. Accelerator modelling and quantitative benchmarking between experiment and numerical simulation becomes feasible. The numerical simulation very much helped us to understand the mechanism of observed beam loss. Also several beam loss mitigation ideas were proposed with a help of numerical simulation and verified by experiment.

REFERENCES

[1] H. Hotchi et al., Phys. Rev. ST Accel. Beams **12**, 040402 (2009).
[2] M. Kinsho, THPWO037 in these proceedings.
[3] H. Hotchi et al., Prog. Theor. Exp. Phys. **2012**, 02B003 (2012).
[4] S. Machida and M. Ikegami, AIP Conf. Proc. **448**, p. 73 (1998).
[5] H. Hotchi et al., Phys. Rev. ST Accel. Beams **15**, 040402 (2012).
[6] F. Tamura et al., Phys. Rev. ST Accel. Beams **12**, 041001 (2009).
[7] M. Yamamoto et al., Nucl. Instrum. Methods Phys. Res., Sect. A **621**, 15 (2010).
[8] Y. Shobuda et al., Phys. Rev. ST Accel. Beams **12**, 032401 (2009).